International Journal of Engineering & Technology, 7 (3.17) (2018) 270-276

International Journal of Engineering & Technology

Website: www.sciencepubco.com/index.php/IJET

Research paper

Time-Averaged Heat Transfer and Vortex Shedding of a Singular and Twin Heated Bluff Bodies in Cross Flow

A. Etminan[1*], A. Sharifian[2], E. Reda[3,4] and Z. Harun[3]

[1]Department of Mechanical Engineering, Faculty of Engineering and Applied Science
Memorial University of Newfoundland
St. John's, NL, A1B 3X5, Canada
[2]School of Mechanical and Electrical Engineering, University of Southern Queensland
Toowoomba QLD 4350, Australia
[3]Centre for Integrated Design for Advanced Mechanical Systems (PRISMA)
Faculty of Engineering and Built Environment
43600 UKM Bangi, Malaysia
[4]Department of Mechanical Engineering, Alexandria University
21544 Alexandria, Egypt
**Corresponding author Email: aetminan@mun.ca*

Abstract

Flow characteristics in the onset of vortex shedding and heat transfer pattern over a single and two same-sized square prisms placed in tandem are studied numerically. All simulations are carried out for Reynolds numbers range varying from 1 to 200 and spacing between the prisms in the order of five widths of prism for in tandem configuration. The calculations are done employing a finite volume in-house computer program according to semi-implicit method for pressure linked equations-consistent (SIMPLEC) numerical procedure and non-staggered mesh in 2-dimensional, steady/unsteady and incompressible flow regimes. The instantaneous and time-averaged streamlines as well as iso-therm pattern for different Reynolds numbers are analysed. Furthermore, the influence of Reynolds number and the onset of vortex shedding on the flow pattern are studied in detail. Three distinct patterns namely fully-attached, trailing-edge separation and leading-edge separation were observed.

Keywords: *Vortex Shedding; Laminar Flow; Heat Transfer; Bluff Body; SIMPELC.*

1. Introduction

Fluid dynamics research on vortex-shedding phenomenon of bluff bodies has attracted a lot of attentions due to its applicability engineering solutions. This event is responsible for the vibration of flexible structures exposed to the flow. Vortex shedding phenomenon enhances time-averaged and instantaneous drag and lift forces meanwhile fluctuations can shorten the endurance limit and strength of exposed structures accordingly. In computational fluid dynamics, vortex shedding depends on the size and the shape of bluff bodies as well as oscillating flow pattern. The different stages of von Kármán vortex street developments were studied by Sharma and Eswaran [1], and Sohankar et al. [2] in details. They showed that a pair of steady symmetric vortices forms in the wake region of buff bodies at low-Reynolds number flow whilst by increasing flow inertia or Reynolds number, the recirculation region behind the cylinder becomes unstable as well as stronger. The commencement of a time-periodic flow from a steady flow can cause eddy shedding is called the Hopf bifurcation. The wake flow of a bluff body is involved in the interaction of an attached shear layer on the frontal side and a considerable downstream wake region as well.

Due to the geometrical shape of an object with square cross section area, it can be considered as a bluff body in flow and makes a massive unsteady wake region in downstream. It is so difficult to predict separated wake and its patterns analytically, experimentally nor numerically. Zdravkovich [3;4] studied the interaction between flow and the solid walls of two cylinders in side-by side configuration in details for steady flow regime. Furthermore, when the space between the cylinders was changed, a variety of flow patterns can be categorized in terms of the behaviour of wake region. The fluid flow characteristics passing an object with circular as well as square cross section areas have been studied quite broadly using numerical and experimental methods by many researchers such as Günter [5], Sarioglu and Yavuz [6] and Sohankar [7] and S. Bhattacharyya and Singh [8]. They found that the flow patterns in the vicinity of two-dimensional more-or-less bluff bodies could be three-dimensional for a wide range of Reynolds numbers and vortex shedding. Additionally, isotherm patterns and fluid structure around an incidence square cylinder has been studied by Etminan et al. [9]. They found a few numerical correlations between some global quantities and the angle of attack as well. The developing of four different unsteady modes of Hopf bifurcation phenomenon in the wake region behind a square cylinder is analyzed by Amalendu [10;11]. He found that the spanwise wake evolved excessively through this nearly symmetrical distributed second mode for considered Reynolds number varyig from 100 to 125.

On the plus side, Dipankar et al. [12-14] numerically studied the forced convective heat transfer in unsteady laminar flow regime around a row of five iso-thermal bars with square cross section area placed in a side-by-side configuration for Reynolds numbers 125 and 150. Their investigation focused on the influence of the gap between the bars on the overall transport phenomena. However, at smaller gap distance, the wake records a very complicated trend resulting in different thermo-hydrodynamic regimes as well. The onset-strip and louvered fins with rectangular cross section area as a periodic, in-line and staggered array has been simulated by Dejong et al. [15] numerically and experimentally. They observed that the Karman vortices have a remarkable impact on heat transfer properties as they continually bring far-field fluid towards the cylinder surface and thereby thinned the local thermal boundary layer. In a recent study, large eddy simulation (LES) approach has been utilized by Harun et al. [16] to show vorticity and different characteristics of flow around larger structures, the Petronas Twin Towers in Kuala Lumpur Malaysia. Flows over the towers in series showed that the vertical activities for the in-between two towers were stronger than in the trailing edge of the second tower. The similarities between both flows around large-scale object as in Harun et al. [16] and small-scale object as in around cylinders lie in the features created behind the objects; show similar characteristics in the recirculation regions.

In the present study, the main purpose is investigating of incoming free-stream flow effects on fluctuating forces and heat transfer quantities over a vast range of Reynolds numbers to achieve several global and instantaneous flow parameters. In summary, in two dimensional laminar flow regime around the square prism, five different flow patterns can be classified; first, creeping steady laminar flow regime with no separation; second, steady flow with separation phenomenon at the trailing edge with a pair of symmetric vortex trapped behind the prism; third, unsteady flow regime with separation located at the trailing edge with vortex shedding; fourth, unsteady flow with separation at the leading edge and reattachment on the sides of the prism; and fifth, unsteady flow with separation at the leading edges with no reattachment on either top or bottom sides of the prism. Furthermore, vortex shedding occurs in the third, fourth, and fifth cases meanwhile the first two cases are steady flows.

It can be shown that vortex shedding can affect all fluid and thermal parameters in computational domain especially in the vicinity of prisms. The considered boundary conditions and geometrical details are illustrated in Figure 1. According to this figure, the dimensionless width of the domain is 20 and the gap distance between the prisms has been assumed as a constant value, i.e. G = 5. These values are chosen according to several comprehensive researchs of the grid generation done by [17- 21].

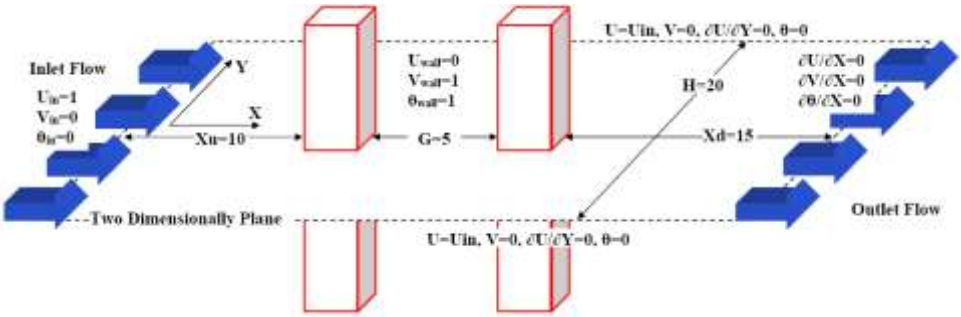

Figure-1: The computational domain and employed boundary conditions for problem under consideration

2. Governing Equations

The non-dimensionl form of governing equations including continuity, Navier-Stokes, and energy equations for unsteady and incompressible flow are given as follows;

$$U_{i,i} = 0 \tag{1}$$

$$U_{i,\tau} + (U_i U_j)_{,j} = -P_{,i} + \mathrm{Re}^{-1} U_{i,jj} \tag{2}$$

$$\theta_{,\tau} + (U_j \theta)_{,j} = (\mathrm{Re}\,\mathrm{Pr})^{-1} \theta_{,jj} \tag{3}$$

where,

$$\tau = \frac{t\,u_{in}}{d}\ ,\ P = \frac{p}{\rho u_{in}^2}\ ,\ U_i = \frac{u_i}{u_{in}}\quad i, j = 1,2\ ,\ \theta = \frac{T - T_{in}}{T_w - T_{in}}$$

The Reynolds, Strouhal and Prandtl numbers are defined as Re = $u_{in}d/\nu$, St = fd/u_{in}, Pr = ν/α. Moreover, u_{in}, d, f, ρ, ν and α correspond to the inlet flow velocity, the width of prisms, frequency of vortex shedding, density, kinematic viscosity and thermal diffusion of fluid respectively. On the plus side, constant density and viscosity and time step, $\Delta\tau$ = 0.025 have been assumed. The local Nusselt number on prisms walls can be determined by Nu = hd/k = $-(\partial\theta/\partial n)_{wall}$, where, h and k are convection and conduction heat transfer coefficients respectively. Furthermore, n is perpendicular direction to the prisms wall.

3. Results

The following parts present, a laminar steady and unsteady-periodic flow regimes with Reynolds number of 1 to 200 is investigated numerically. For covering all essential and transient phenomena, flow simulations have been done for numerous Reynolds number. The distance between the prisms is fixed at five widths of the prisms. Eventually, flow structure and heat transfer are studied in details, where the onset of vortex shedding occurred in the range of Reynolds number, 45-50 for single prism geometry.

3.1 Single Square Prism

After a transient process, a fully time-periodic flow can be found when a constant domain of fluctuating forces is observed. All global parameters have been computed over at least 20 completed eddy-shedding cycles. Furthermore, grid independency study has been done by Sohankar and Etminan [17] where a comprehensive data are provided for all computational distances as well.

Based on a numerical linear stability analysis done by Kelkar and Patankar [22], the onset of vortex shedding around a square cylinder was equal to 53 by performing at a blockage ratio of 14.3%. However, Sohankar et al. [23] determined its value about 47±2 for the practically zero-blockage experiments. Sohankar et al. [18] also found Re number corresponded to the onset of vortex shedding to be 51.2±1 for blockage ratio equal to 5%. Sharma and Eswaran [1] also determined the range of critical Reynolds number for single square cylinder as Re=45-50 whilst in the present study, the symmetric wake behind the prisms is formed for Re=45 and eddy shedding is occurred for Re > 45. Therefore, a critical

Reynolds number can be assessed approximately between 45 and 50 (see Figure 2). For Reynolds numbers greater than the critical Reynolds number (Re ≥ 50), a pair of unstable vortexes, an unsteady-periodic wake and a von Kármán vortex street are formed behind the square prism consecutively. Figure 2 shows the instantaneous streamlines coloured by temperature distribution around prism for different Reynolds numbers. This figure illustrates a crowding of isotherm pattern just in regions near the solid wall of cylinder where the separation is not seen. The highest crowding of the isotherm lines around the body indicating the highest Nusselt number which is found on the frontal face, where the thermal boundary layer growth meanwhile the minimum crowding of the isotherms is observed on the rear face.

Figure 3 illustrates the time-averaged streamlines coloured by non-dimensional pressure above horizontal axis at Y=0 and streamlines coloured by non-dimensional temperature below the horizontal axis for different Reynolds numbers. The attached shear layer to the frontal side of prism is bifurcated into the two-shear layers sticking to the top and bottom walls. These shear layers are separated from the leading corners of prism and reattach to the top and bottom walls for Reynolds number greater than 120. For higher value of Reynolds number, the separation point location moves into the downstream exactly at the trailing corners of the prism. The intensity of isotherms around the prism becomes more non-uniform, when the Reynolds numbers increases. The circulating region length also decreases in size versus Reynolds number.

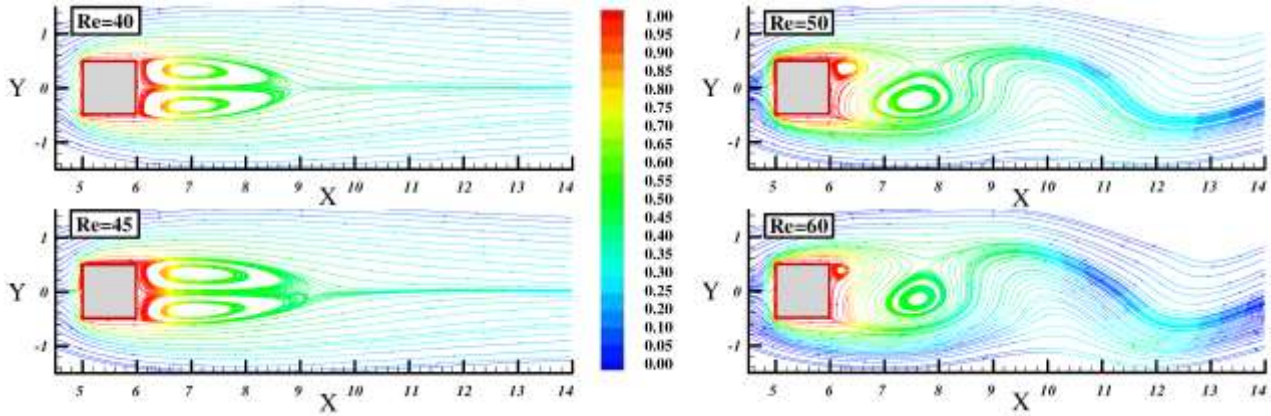

Figure-2: The instantaneous streamlines coloured by dimensionless temperature in the vicinity of single prism for different Reynolds number

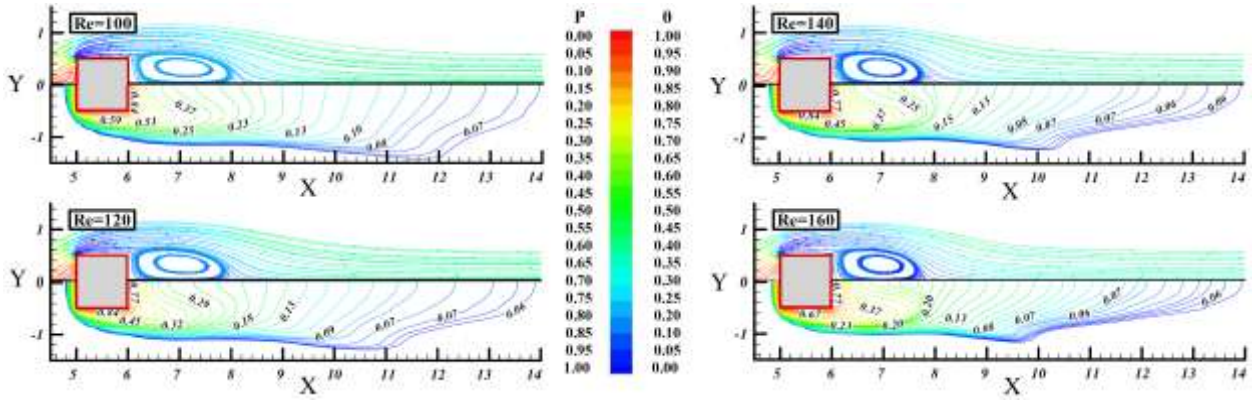

Figure-3: The time-averaged streamlines coloured by dimensionless pressure above horizontal axis and isotherm patterns below horizontal axis in the vicinity of single prism for different Reynolds number

The drag coefficient and total Nusselt number are compared with some experimental and numerical results in Figure 4. As can be observed, the average Nusselt number on the top and the bottom sides of the prism are similar and the deviation between the calculated Nusselt numbers and the available others' result is negligible. The maximum difference between the total Nusselt numbers is about 4.2% and this deviation decreases to an amount of 0.4% when Reynolds number goes up. As it can be seen in Figure 4, there is a reasonable agreement between the present results and the others' and the small deviations between results are expected due to the different grid size, considered time step, solver algorithm and so forth.

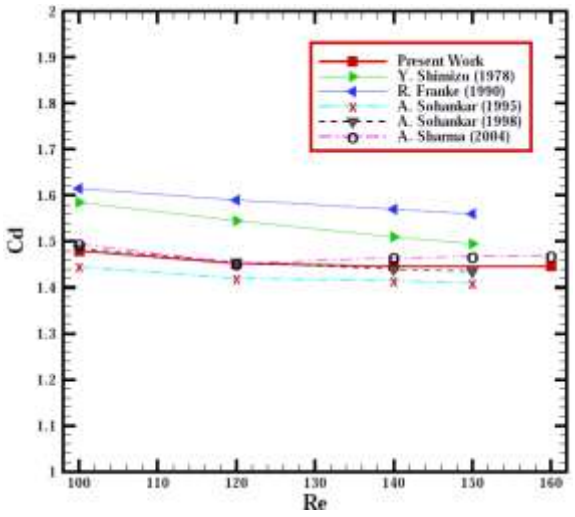

(a)

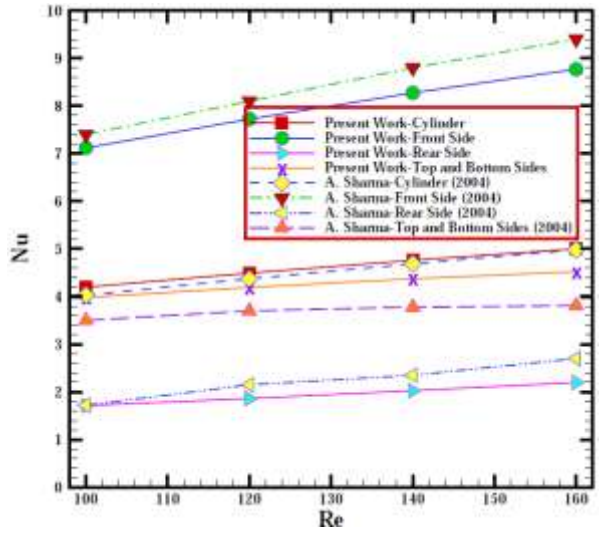

(b)

Figure-4: The variation of (a) drag coefficient and (b) Nusselt number versus Reynolds number

3.2 Single Square Prism

In all simulations, the fluid flow structure and the heat transfer characteristics have been computed over almost 20 fully eddy-shedding cycles exactly similar to single prism case. Regarding the nature of periodically flow in the fully developed case, the lift and drag force signal amplitudes are reached approximately to constant levels with a specific and constant fluctuations.

The time-averaged streamlines around the upstream prism are plotted in Figure 5. It is found that for Re=100, the flow separation point is located on the trailing edge, while for higher Reynolds numbers, this point is moved towards the leading edge and eddy regions are just about to form on the top and bottom sides of upstream prism. As Reynolds number increases, separation point would be placed on leading edge, the flow is separated, eddy regions are formed, and flow is attached to the top and bottom sides again. By increasing the Reynolds number, rotational regions are connected to the wake regions behind the upstream prism and eddy regions propagated in cross flow direction whilst the flow separation point of downstream prism is always on trailing edge.

Figure 6 depicts the time history of the instantaneous X and Y-velocity components at three specified locations i.e. on the top side, rear-top corner and rear side of prisms numbered 1, 2 and 3 respectively for Re = 100 obviously. The non-dimensional vertical distance of considered points from the prism walls is 0.03. In all the cases, because of upstream prism effect on the downstream, the domain of fluctuating forces exerted on downstream prism is wider than corresponding values of the upstream one. In the wake region behind the prisms due to eddy formation, the fluctuations of flow parameters, such as velocity components as well as temperature is less than other regions around the prisms. Furthermore, the eddy formation regions behind the prisms and vortex regions sticking to the up side of prisms caused the highest fluctuation at point number 2 than other points.

As mentioned before, the flow remained steady state between Re=1 and Re=35, then it is changed to unsteady-periodic regime. On the other hand, symmetric flow would be converted to asymmetric-periodic flow for a critical Reynolds number. As a simplification for describing the physics of flow in the vicinity of objects in the following graphs the front, top, rear, and bottom sides are labeled AB, BC, CD, and DA respectively. Pressure distribution on the solid surfaces of the prisms are carried out for evaluating the influence of change in Re for both considered steady and unsteady flow regimes.

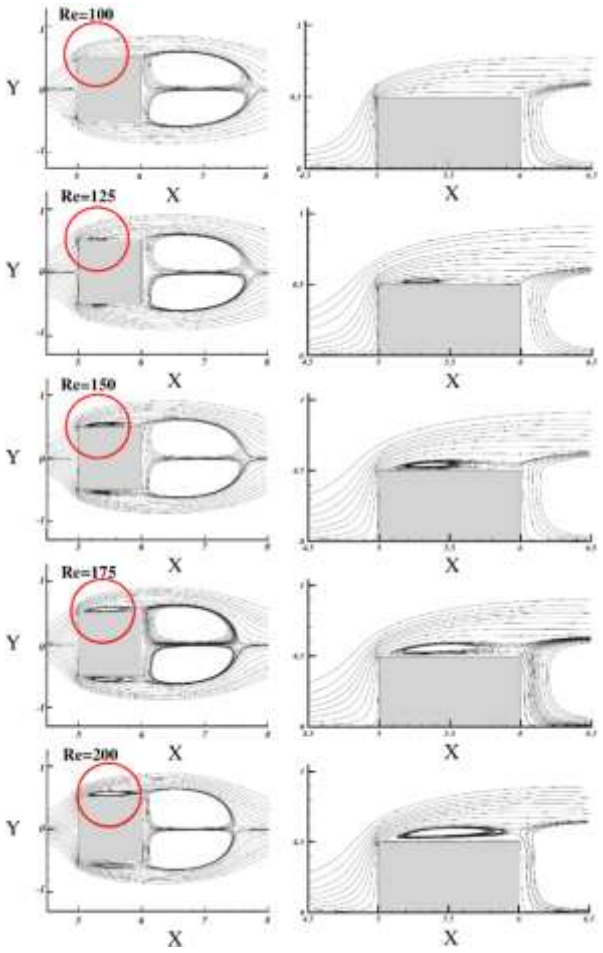

Figure-5: The time-averaged streamlines around the upstream prism (left-hand side graphs) and zoomed out area (right-hand side graphs) for different Reynolds numbers

Figure 7 depicts the pressure coefficient distribution in the vicinity of the prisms for different Reynolds number where the pressure coefficient can be calculated by $Cp = p/(\rho u_{in}^2/2)$. It can be seen that Reynolds number has no remarkable impact on the pressure coefficient distribution on the upstream solid wall of cylinders. When Reynolds number is low, the deviation of pressure coefficient distribution on prisms walls would be related to the change of the distance required for providing eddy formation in the wake regions of the prisms and the strength of the formed vortices as well.

It can be observed that due to stagnation flow exactly on the upstream walls of the prisms, the value of pressure coefficient on them is maximum. Moreover, by increasing flow inertia, Cp is jumped abruptly between Re=1 and Re=10 and separation occurs on both prisms. Since, the distance between the prisms is filled up by the wake region for Re=50, the pressure coefficient distribution on the downstream prism walls becomes negative.

Figure 8 depicts the Nusselt number distribution in instantaneous, time-averaged and unsteady-periodic flows on the prisms to comprehend the effects of different Reynolds numbers on heat transfer pattern. It can be found that the Reynolds number has most significant impact on the Nusselt number distribution, in particular, on the front side. Since no vortex shedding is occurred in steady flow regime, flow pattern between the prisms is remained symmetric and the lowest heat transfer rate occurs on the rear side of prisms. The same trend is also observed for unsteady-periodic flow regime. The difference in Nusselt number distribution on prisms walls for lower Reynolds number is related to the distance between the prisms, vortex formation and the strength of the formed vortices as well. It seems that the level of Nusselt number at stag-

nation point is the lowest. In addition, a leap is observed in the Reynolds number ranging from 1 to 10 for Nusselt number distribution due to the flow inertia increasing and separation occurring for both prisms. Furthermore, the wake region between prisms does not allow flow to mix into downstream flow in particular for Re=50, and Nusselt number distribution on the frontal side of downstream prism would be substantially lower in comparison with other sides accordingly.

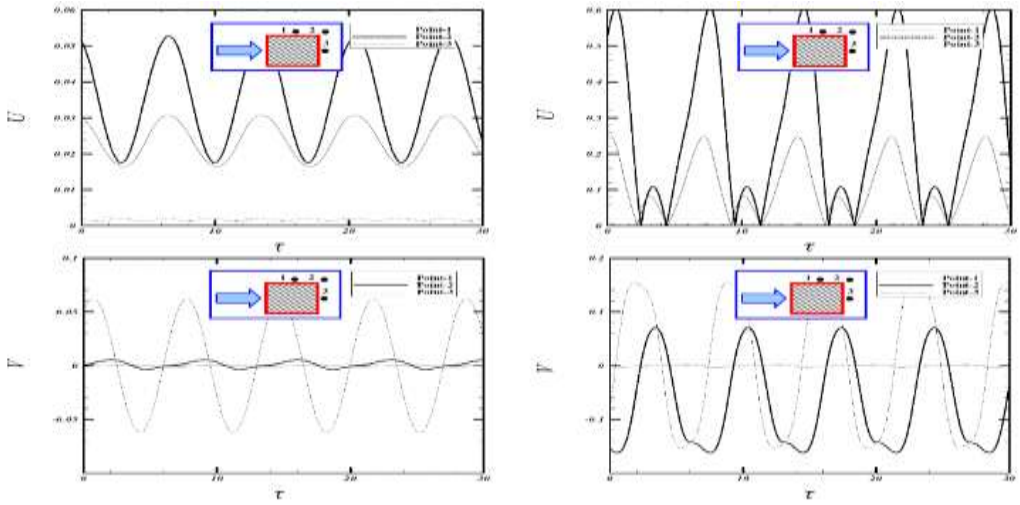

Figure-6: The time history of instantaneous velocity components at three defined points adjacent to upstream prism (left-hand side graphs) and downstream prism (right-hand side graphs) for Re = 100, G = 5

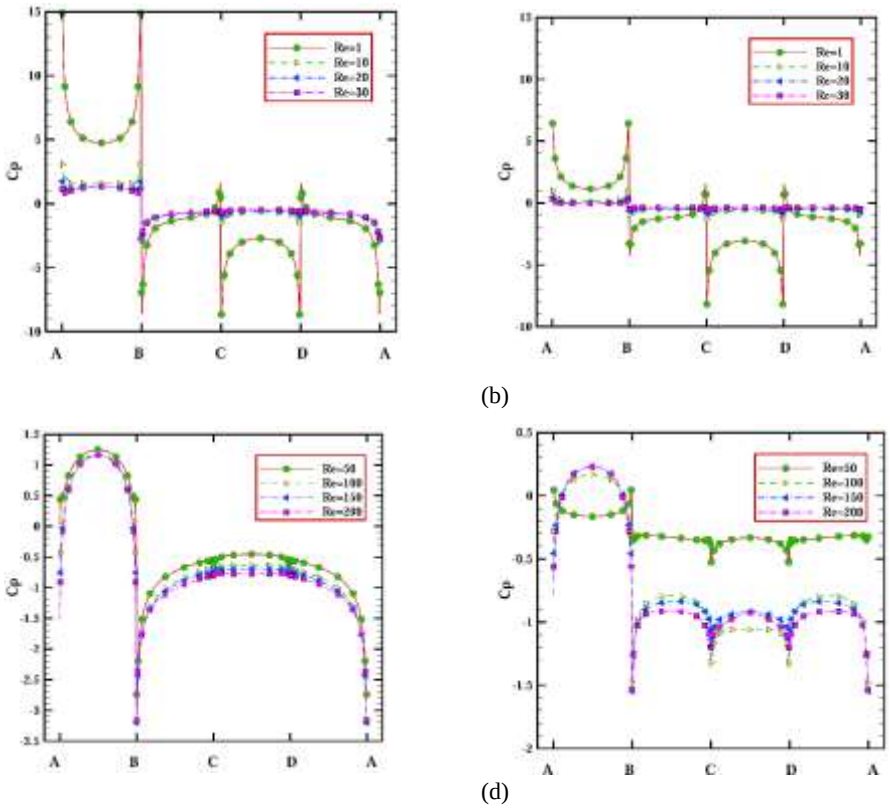

(a) (b)

(c) (d)

Figure-7: The pressure coefficient distribution on upstream prism (left-hand side graphs) and downstream prism (right-hand side graphs) for different Reynolds numbers in (a, b) steady flow and (c, d) unsteady-periodic flow

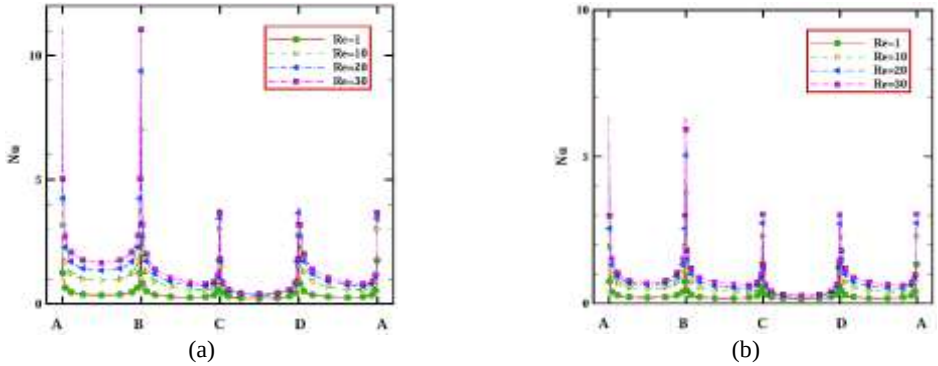

(a) (b)

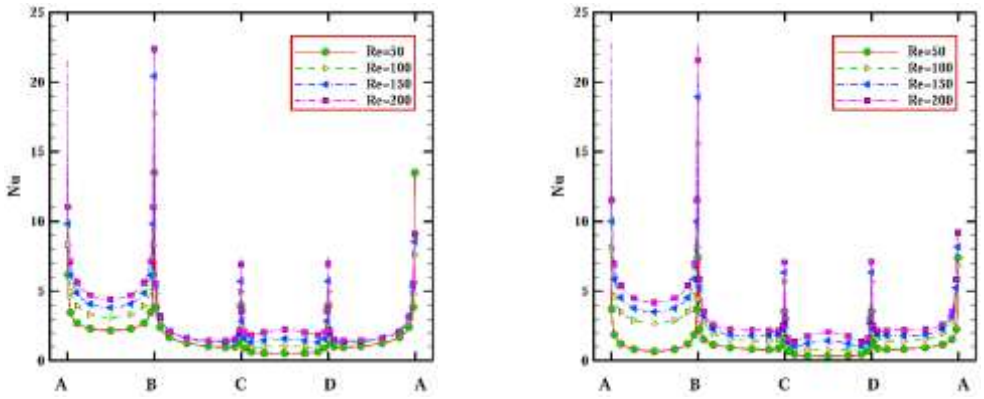

(c) (d)

Figure-8: The Nusselt number distribution on upstream prism (left side graphs) and downstream prism (right side graphs) for different Reynolds numbers in (a, b) steady flow and (c, d) unsteady-periodic flow.

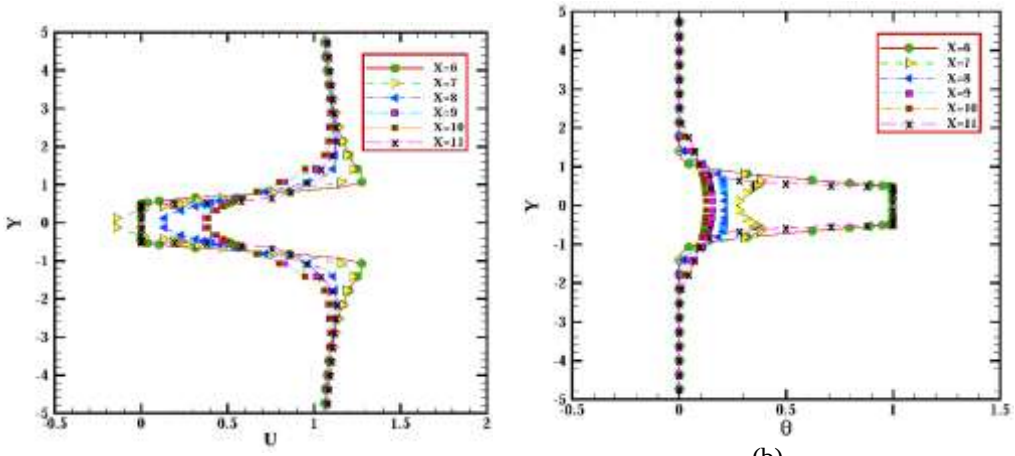

(a) (b)

Figure-9: The distribution of (a) X-velocity component and; (b) dimensionless temperature, at the six sections between the prisms for Re = 100, G = 5

When Reynolds number or the flow inertia goes up simultaneous with reduction of the recirculation length behind the upstream prism give a longer opportunity for the flow to recovers its pressure and transfers heat flow to the cold stream and loses its temperature before encountering the downstream prism. The X-velocity component and temperature at the six sections in the gap distance between the prisms in Figure 9 are illustrated for Re=100 and a fixed-gap between the prisms, G=5.

According to Figure 9, the flow is attached to the prisms walls for the sake of the wall-shear effect. Therefore, the magnitude of X-velocity component becomes zero and dimensionless temperature becomes equal by solid wall temperature of prisms at X=6 and X=11. The negative sign of X-velocity component denotes reverse flow due to the vortices behind the upstream prism. At further distance away from the prisms and their vortices, the velocity and temperature of flow change to the inlet uniform flow conditions. The highest temperature is related to the wake region in the vicinity of the upstream prism. It is not only due to the prism's heated-wall, but also because of flow pattern and temperature gradient intensity. Moreover, cold flow has more influence over temperature distribution by keeping out of wake region between the prisms. On the plus side, the X-velocity component and temperature values on the considered lines got the free stream conditions outside of gap region quickly.

4. Conclusion

In this paper, we attempt to carry out an in-detail study on the features of an unconfined flow around single and two in-tandem objects with square cross section area in both steady and unsteady-periodic flow regimes. A critical Reynolds number has been found to be approximately between 45 and 50 for single and 35 and 40 for in tandem cases. With regarding the location of separation points, three different onset values had been suggested; the first one is the onset of separation occurs between Reynolds number 1 and 2; the second case is the onset of vortex shedding phenomenon with separation point at the trailing-edge for Reynolds number between 35 and 40; and the third is the onset of separation at the leading-edge of prism which occurs for Reynolds number between 100 and 125 meanwhile the flow separation point of downstream prism is always on trailing edge. Furthermore, it is observed that the magnitude of the fluctuating forces exerted on the downstream prism is significantly larger than the corresponding values of upstream prism due to the flow interaction in the gap space. Besides, pressure coefficient and Nusselt number distributions on downstream prism for Reynolds numbers varying from 55 to 60 are risen dramatically due to the change of the flow pattern in the gap between the prisms. On the other hand, it is perceived that the Nusselt number on the front, top and bottom, and rear sides, have highest, intermediate, and lowest values respectively.

Acknowledgement

The authors would like to thank Universiti Kebangsaan Malaysia (UKM) for grant Fundamental Research Grant Scheme code FRGS/1/2016/TK03/UKM/02/1.

Nomenclature

English Letter

Cd	total drag coefficient
Cdf	viscous drag coefficient
Cdp	pressure drag coefficient
Cp	pressure coefficient
d	width of square prisms
f	frequency of vortex shedding
G	spacing between the prisms
h	convective heat transfer coefficient
k	fluid thermal conductivity coefficient
n	normal direction on prisms walls
Nu	Nusselt number
p	Pressure
P	non-dimensional pressure
Pr	Prandtl number
Re	Reynolds number
St	Strouhal number
t	time
T_{in}	free stream temperature
T_w	prism wall temperature
u	stream wise velocity
U	dimensionless stream wise velocity
u_{in}	free stream velocity
v	cross-stream velocity
V	dimensionless cross-stream velocity
x	stream wise dimension coordinate
X	non-dimension stream-wise coordinate, (=x/d)
Xd	dimensionless stream wise distance between the rear side of the downstream prism and the exit plane
Xu	dimensionless stream wise distance between the inlet plane and the frontal side of the upstream prism
y	cross-stream dimension of coordinate
Y	non-dimension cross-stream coordinate, (=y/d)

Greek Letter

α	thermal diffusion coefficient
θ	dimensionless temperature
ρ	fluid density
τ	dimensionless time
ν	fluid kinematic viscosity

References

[1] Sharma, A. and Eswaran, V. (2004), Heat and Fluid Flow across a Square Cylinder in the Two Dimensional Laminar Flow Regime. Numerical Heat Transfer, Part A: Application 45, 247-269.

[2] Sohankar, A., Davidson, L. and Norberg, C. (1995), Numerical Simulation of Unsteady Flow Around a Square 2D Cylinder. The 12th Australasian Fluid Mechanics Conference, Bilger RW (ed.) 517-520.

[3] Zdravkovich, M.M. (1997), Flow around Circular Cylinders, Oxford University Press, NewYork.

[4] Zdravkovich, M.M. (1985), Flow-Induced Oscillations of Two Interfering Circular Cylinders. Journal of Sound and Vibration 101, 511-521.

[5] Günter, S. (2001). Reynolds Number Effects in Flow Around more-or-less Bluff Bodies. Journal of Wind Engineering and Industrial Aerodynamics 89, 1267-1289.

[6] Sarioglu, M. and Yavuz, T. (2002) Subcritical Flow Around Bluff Bodies. AIAA 40(7), 1257-1268.

[7] Sohankar, A. (2006) Flow Over a Bluff Body from Moderate to High Reynolds Numbers Using Large Eddy Simulation. Computers and Fluids 35, 1154-1168.

[8] Bhattacharyya, S., Singh, A. K. (2010) Vortex shedding and heat transfer dependence on effective Reynolds number for mixed convection around a cylinder in cross flow. International Journal of Heat and Mass Transfer 53(15-16), 3202-3212.

[9] Etminan, A., Harun, Z. and Gharehchahi, H.R. (2014) Determination of Fluid Flow Characteristics and Pattern of Heat Transfer around a Prism at Incidence. Ciência e Técnica Vitivinícola Journal 29 (12), 141-157.

[10] Amalendu, S. (2009) Hopf Bifurcation in the Wake of a Square Cylinder. Physics of Fluids 21(3), 105-124.

[11] Amalendu, S. (2010) Hopf Bifurcation in Bluff Body Wakes. The 5th International Symposium on Computational Wind Engineering, Chapel Hill, North Carolina, USA.

[12] Dipankar, C., Gautam, B. and Sakir, A. (2010), Numerical Simulation of Flow Past Row of Square Cylinders for Various Separation Ratios. Computers and Fluids 39(1), 49-59.

[13] Dipankar, C., Gautam B, Sakir A. (2012), Mixed Convection Heat Transfer from an In-Line Row of Square Cylinders in Cross-Flow at Low Reynolds Number. Numerical Heat Transfer, Part A: Application 61(12), 891-911.

[14] Dipankar, C., Bittagopal, M. (2013), Effect of thermal buoyancy on vortex shedding behind a square cylinder in cross flow at low Reynolds numbers. International Journal of Heat and Mass Transfer 54(25-26), 5262-5274.

[15] Dejong, N.C., Zhang, L.W., Jacobi, A.M., Balachandar, S. and Tafti, D.K. (2010) A Complementary Experimental and Numerical Study of Flow and Heat Transfer in Offset Strip-Fin Heat Exchangers. Journal of Heat Transfer 120, 690-698.

[16] Harun, Z., Reda, E. and Abdullah, S. (2015), Large Eddy Simulation of the Wind Flow over Skyscrapers, Recent Advances in Mechanics and Mechanical Engineering, 72-79.

[17] Sohankar, A. and Etminan, A. (2009) Forced-Convection Heat Transfer from Tandem Square Cylinders in Cross Flow at Low Reynolds Numbers. International Journal for Numerical Methods in Fluids 60, 733-751.

[18] Sohankar, A., Norberg, C. and Davidson, L. (1998) Low-Reynolds-Number Flow Around a Square Cylinder at Incidence: Study of Blockage, Onset of Vortex Shedding and Outlet Boundary Condition. International Journal for Numerical Methods in Fluids 26, 39-56.

[19] Etminan, A., Moosavi, M. and Ghaedsharafi, N. (2011), Determination of Flow Configurations and Fluid Forces Acting on two Tandem Square Cylinders in Cross Flow and its Wake Patterns. International Journal of Mechanics 5, 63-74.

[20] Etminan, A. and Barzegar, A. (2012) Instantaneous and Time-Averaged Flow Structure around two Heated Square Cylinders in the Laminar Flow Regime. Applied Mechanics and Materials Journal 110-116: 2898-2902.

[21] Etminan, A. (2013) Flow and Heat Transfer over two Bluff Bodies from Very Low to High Reynolds Numbers in the Laminar and Turbulent Flow Regimes. International Journal of Advanced Design and Manufacturing Technology 2(6), 61-72.

[22] Kelkar, K.M.K.M. and Patankar, S.V. (1992), Numerical Prediction of Vortex Shedding behind a Square Cylinder," International Journal of Numerical Methods in Fluids 14, 327-341.

[23] Sohankar, A., Norberg, C. and Davidson, L. (1997) Numerical Simulation of Unsteady Low- Reynolds Number Flow around Rectangular Cylinders at Incidence. Journal of Wind Engineering and Industrial Aerodynamics 69, 189-201.

[24] Shimizu, Y. and Tanida, Y. (1978), Fluid Forces Acting on Cylinders of Rectangular Cross Section. Transactions of the Japan Society of Mechanical Engineering 44, 2699-